Colloid Polym Sci 274:1119–1128 (1996)

ORIGINAL CONTRIBUTION

V.N. Kalashnikov
M.G. Tsiklauri

Supermolecular structures and flow birefringence in polymer solutions

Received: 9 January 1996
Accepted: 3 June 1996

Dr. V.N. Kalashnikov (✉)
M.G. Tsiklauri
Institute for Problems in Mechanics
Russian Academy of Sciences
Prospect Vernadskogo 101
Moscow 117526, Russia

Abstract Experimental studies of supermolecular structures and localized flow birefringence in solutions of high-molecular weight polymer are described. Advantage is taken of poly(ethylene oxide) and polyisobutylene. Supermolecular structures are examined with the aid of optical microscopy using freeze-dried samples of the polymer solutions. Birefringence is investigated that arises in planar elongational flow in a cross-slot cell. Flow velocities at which the onset of the localized birefringence occurs are determined. Then these velocities are correlated with viscoelastic characteristics of the solutions. The presence of a liquid–crystalline fibrillar network in the polymer solutions exhibiting flow birefringence is ascertained. The fibrils are birefringent objects. The localized birefringence phenomenon is explained in term of the orientation of the fibrils in elongational flow. It has been shown that the onset of localized birefringence occurs at a critical Weissenberg number, the value of which is close to unity.

Key words Birefringence – fibrillar network – Weissenberg number

Introduction

Solutions of high-molecular weight polymers are known to acquire optical anisotropy in flow. Orientational effects arising in hydrodynamic fields result in a birefringence phenomenon. Previously, investigations on flow birefringence were mostly limited to shear flow [1]. In this type of flow orientational effects and birefringence are rather weak. Orientational phenomena in a flow with a positive longitudinal velocity gradient are much more pronounced. Under these circumstances dynamic birefringence is of a particular character. In flow regions, where the strain rates are sufficiently large, localized domains of optical anisotropy appear which can be observed as thin bright lines between crossed polarizers. Localized birefringence was first detected in the hydrodynamic field between two opposite coaxial orifices as a consequence of two opposed jets [2]. This phenomenon was further investigated in planar elongational flow. Such a flow was realized in devices with rotating cylinders [3–6], in cross-slot devices [7] and also close to obstacles of various profiles [8]. A characteristic feature of the localized flow birefringence is its threshold nature. Birefringence arises when the extension rate of the liquid elements reaches significant values [9]. In addition to the strain rate, the concentration and the molecular weight of the dissolved polymer are of importance. Dynamic birefringence can only be observed for sufficiently high concentrations and molecular weights [5, 7].

In many cases, localized birefringence is accompanied by flow-induced crystal formation in the regions where optical anisotropy shows its steep ascent [2, 10–12]. Depending on the solution temperature, the concentration and the molecular weight of the polymer, stable solid crystallites as well as liquid–crystalline structures can be formed in elongational flow as a result of the orientation effect. After cessation of flow the liquid–crystalline structures disappear within a finite time span.

Colloid & Polymer Science, Vol. 274, No. 12 (1996)

The interpretation of flow birefringence depends on an insight into the nature of solutions of high molecular weight polymers. A point of view is presently widely encountered in polymer science according to which the forces of attraction between the macromolecular chains in solutions are deemed negligibly small and thus the possibility of the formation of supermolecular structures in these solutions at rest is disregarded. It is assumed that for dilute solutions, satisfying the condition $c < c^* = 1/[\eta]$, where c is the weight concentration and $[\eta]$ is the intrinsic viscosity at low shear rates, the polymer is dispersed in the solution in the form of discrete macromolecular coils. When the concentration of macromolecules exceeds c^*, where the coils certainly touch each other, the chains are supposed to be entangled. A birefringence phenomenon is considered to be the consequence of the deformation and orientation of macromolecules. It is just these objects that are thought of as primary birefringent elements. In particular, in elongational flow the coils are assumed to be extended and predominantly oriented along the stream lines.

However, data are available that support the existence of supermolecular structures which arise in solutions, even though $c \ll c^*$, as a result of attraction forces between the sufficiently long polymer chains.

Aggregation of the macromolecules has been proposed for explaining the differences which are observed in the measured molecular weights on changing the solvent or the temperature of the solution. Analogous interpretations were required by light scattering experiments, which in the case of high molecular weight polymers gave values of M that exceeded the real values by several orders of magnitude [13]. Macromolecular aggregation in polymer solutions at very high dilutions was considered in works [14–17] in connection with turbulent drag reduction. Certain flow birefringence data testify, in the view of the authors of work [18], that entanglements occurred at concentrations much below c^*, namely, at c as low as $c^*/50$. Investigations of the elastic properties of dilute solutions of high molecular weight polymers led to results which differ significantly from the predictions of the theories that assume molecular dispersity of polymer [19]. A similar situation exists with regard to results of viscosity measurements [20].

The detailed structure of polymer solutions can be inferred from data of electron and optical microscopy. The observations show that macromolecular aggregates more often than not, exist in the solutions of high-molecular weight polymers [21–28]. Specific approaches are required to observe the discrete macromolecules of such polymers. In particular, in ref. [23] molecules were isolated by dispersing a dilute solution of the polymer as fine droplets onto a substrate, so that each droplet contained no more than one polymer molecule. In addition to that, the solution was a mixture of two solvents, a good one and a poor one. Even so, cross-linking could not be fully eliminated for certain polymers. Continuous three-dimensional networks of long fibrils are often noticed in the solutions [25–28]. The fibrils consist of many macromolecules and on numerous occasions have thickness sufficient to be easily observed by optical means without the use of electron microscopy.

It was supposed in our paper [28] that the flow birefringence of polymer solutions is connected with the existence of fibrillar networks. This is a subject we elaborate upon in the present work. The experiments were undertaken in two ways: On the one hand, the structures of polymer solutions were examined with the aid of optical microscopy. On the other hand, flow velocities at which the onset of the localized birefringence occurs in cross-slot flow were determined for different polymer–solvent systems, concentrations and temperatures, and these velocities then were correlated with viscoelastic characteristics of the solutions.

Experimental methods

Microscopy

Freeze-dried samples were employed for investigation of structures in polymer solutions. Commercially available vacuum apparatus for the preparation of specimens was used. This apparatus made it possible to carry out vacuum treatments down to 1–0.1 mPa. The sample under the treatment was mounted on a metal stage within a chamber of the apparatus. The stage was provided with a thermocouple. If desired, the stage of the vacuum chamber could be cooled by a liquid nitrogen supplied from the outside. Two methods of removing the solvent under vacuum were used: with preliminary freezing of the solution by liquid nitrogen (slow drying), and without preliminary freezing (rapid drying).

In the method of slow drying a thin glass plate (a cover glass) was mounted on the bottom of the cavity of copper container filled with the liquid nitrogen. A small droplet of the solution was allowed to fall into the cavity and the container was then transferred onto the precooled stage of vacuum chamber. The vacuum pump was switched on, the liquid nitrogen quickly evaporated from the container, after which the sublimation of the frozen solvent began. This process occurred at sufficiently low temperature. Specifically, the sublimation of the aqueous solutions was carried out at the temperature close to $-80\,^{\circ}C$. A period of 8–10 h was required for the complete volatilization of the water molecules.

In order to carry out the rapid drying procedure the thin glass plate supporting a droplet of solution was placed

in the vacuum apparatus. Extra cooling of the camera stage by supply of liquid nitrogen was not carried out. As a result of the intense evaporation of the solvent the droplet freezes in quickly. By using a thermocouple it was shown, in particular, that the frozen droplets of water solution in the process of sublimation could be self-cooled to $-35\,^{\circ}C$. At such not-too-low temperatures the sublimation of the solvent occurred quite rapidly. After a lapse of about 1 h the frozen droplets died.

When the sublimation was complete, the polymer residues on the glass plates were slowly warmed up to room temperature under vacuum. Finally the samples were removed to be observed under the optical microscope.

Flow birefringence

The onset of localized birefringence was observed in the planar elongational flow created in a cell consisting of two narrow intersecting channels of equal width forming a rectangular cross. The flow rates in the arms of the cross are the same. The two entering flows of opposite direction meet in the center of the cross and are let out through the two other branches. The design of such a cross-slot cell was first reported in ref. [7].

We used two cells. In the first cell, the channel width was $d = 0.49$ mm, its depth $h = 15$ mm; the second cell was characterized by $d = 0.80$ mm, and $h = 26$ mm. The optical part of the arrangement consisted of a light source (a mercury lamp), a collimator and a microscope with polarizers. The cell was installed on the microscope stage. The center line of the cross coincided with the optical axis. The angle between the plane of polarization of the entering light beam and the direction of the channels was 45°. This ensured the maximum intensity of light passing through the analyzer because of flow birefringence effect. The upper and lower lids of the cell contained windows made of polished optical glass.

The solution was supplied from a temperature-controlled head tank. The liquid temperature was checked by thermometers at the inlet and outlet sections of the system. The flow rate could be regulated by a valve at the outlet. At the instant the birefringent region became visible to the eye through the microscope in the course of increasing the flow rate, the last was measured by a volumetric method. For the same solution, measurements were repeated several times to ensure sufficient reliability.

Solutions and their rheological properties

The experiments were carried out with solutions of poly(ethylene oxide) (PEO) and polyisobutylene (PIB). As solvents, water and isopropanol for PEO and kerosene and hexane for PIB were used. The PEO samples were produced by Union Carbide Corp. and Meisei Chemical Co., as well as within Bulgaria. The samples from Union Carbide Corp. were Polyox WSR-301 (the intrinsic viscosity at low shear rate in water $[\eta] = 2500$), Polyox WSR-205 ($[\eta] = 790$), Polyox WSR-N750 ($[\eta] = 450$), and Polyox WSR-N10 ($[\eta] = 90$). The sample from Meisei Chemical Co. under the name Alcox exhibited the highest intrinsic viscosity $[\eta] = 4500$. The sample from Bulgaria under the name Badimol possessed in water $[\eta] = 1000$. The PIB sample was Russian-made polymer with intrinsic viscosity at low shear rate in kerosene $[\eta] = 950$.

The power relationships are commonly used in order to calculate the molecular weights from the intrinsic viscosities. As a rule, the magnitudes of empirical constants for these relationships are determined by light-scattering measurements, in which the polymer substance is considered to be molecularly dispersed in solution. The accuracy of this method significantly decreases when supermolecular aggregates are present. Therefore the molecular weights are not reported in our work, while we assume that their values increase with increasing $[\eta]$.

Besides the zero-shear-rate intrinsic viscosity, viscosity at various shear rates and the natural time [29] (i.e., relaxation time of elastic stresses which manifests itself at low disturbance frequencies) were determined. Viscosity was measured by means of viscometers described in work [20]. Determination of the natural time was conducted by measurement of the mean velocity at the onset of the elastic turbulence in flows through channels with periodically varying cross-sections [19]. It was found that the elastic turbulence arises in these channels at the certain critical Weissenberg number, the value of which was determined [30]. Therefore, the natural time could be calculated using the mean velocity obtained in experiments and the known values – the characteristic channel size and the critical Weissenberg number.

Results of conducted tests were consistent with those in just mentioned works. Shear-thinning and appreciable elastic properties of the solutions came into existence at some critical intrinsic viscosity of the dissolved polymer. This critical value of $[\eta]$ for PEO in water approximated 280 at not-too-high concentrations. The natural time θ of the PEO–water and PIB–kerosene solutions was proportional to the 1/2 power of the polymer concentration. This proportionality was valid over a wide range of concentrations up to several parts per thousand. In addition to results of work [30], deviations from mentioned proportionality were detected for high concentrations exceeding $5 \cdot 10^{-3}$ for PEO in water. Usual correlation $\theta \sim c^{1/2}$ and departure from this proportionality for high concentration

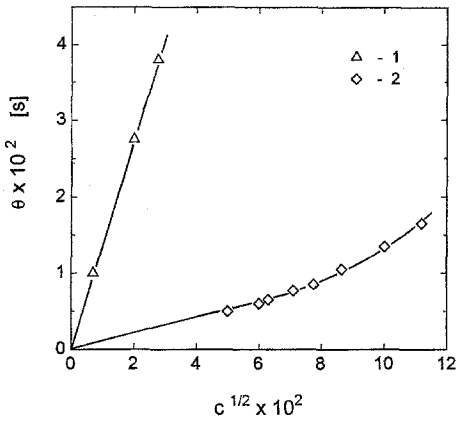

Fig. 1 Natural time as a function of the concentration to the one-half power for aqueous solutions of PEO. 22 °C. $[\eta] = 2500$ (1), $[\eta] = 790$ (2)

Table 1 The values of $\theta \cdot c^{-1/2}$ for the polymer solutions, used in the flow birefringence tests

	PEO + water					PIB + kerosene
$[\eta]$		2500		1000	790	950
Temperature, °C	8.6	22.0	41.7	22.0	22.0	22.0
$\theta \cdot c^{-1/2}$, s	1.60	1.37	0.62	0.56	0.10	0.49

range can be illustrated with the curves in Fig. 1. Averaged values of $\theta \cdot c^{-1/2}$ for $c < 5 \cdot 10^{-3}$ are given in Table 1.

Results

Supermolecular structures

A study of the samples of the polymer residues under the microscope led to the conclusion that, in line with the findings in works [25–27], a network of supermolecular structures can exist even in very dilute solutions of high molecular weight polymers. The network is formed by fibrils consisting of a large number of macromolecules. As concentration increases, the network becomes more dense, while the thickness of the fibrils changes only a little. Shown in Fig. 2 are micrographs of Polyox WSR-301 samples as obtained from solutions of different concentrations, the thickness of fibrils for all cases ranges up to about 1 μm. The same thickness of fibrils are observed in the micrographs of samples derived from the water solutions of PEO in works [25–27]. The size of the network cells and the lengths of separate fibrils diminish with increasing concentration. The fibrillar network is observed at concentrations which are considerably smaller than $c^* = 4 \cdot 10^{-4} = 400$ ppm for the polymer used.

The fibrils are the birefringent structures. This is confirmed by the observation of the polymer residues between crossed polarizers (Fig. 2d). When rotating the stage of the microscope between the crossed polarizers, one observes a change in the illumination intensity for the fibrils. Depending on the orientation, the fibrils can either be nicely observable against the dark background or completely extinct. (See Fig. 3.)

The micrographs in Fig. 4 present the samples obtained from aqueous solutions containing at a single concentration $c = 10$ ppm PEOs of various intrinsic viscosities (molecular weights). It can be seen that for a small intrinsic viscosity $[\eta] = 90$ the aggregation of the macromolecules leads to the formation of limited number of globular particles up to 2 μm size rather than a continuous network. The trend has been noticed toward the generation of the network in the solution of PEO having $[\eta] = 450$. The fibrillar network becomes more dense with further growth of the intrinsic viscosity.

We also carried out observation of the samples that were prepared from the water solutions of PEO degraded partially or fully at turbulent regime in a rotational apparatus with coaxial cylinders that was used in work [31] for the investigation of drag reduction. The degree of degradation was judged from the drag reduction decay. During degradation, the network became sparser. Ultimately, the network dies out and the globular particles appear in the micrographs, much as the globular particles appear with decreasing intrinsic viscosity of dissolved polymer in Fig. 4d. This takes place when drag reduction ceases and the destruction arrests itself at the certain molecular weight of polymer. Under these conditions shear-thinning and elasticity of the solution disappear. Prolongation of exposure to the turbulent flow leaves viscosity of the solution and consequently molecular weight of the polymer unaltered. The limiting value of intrinsic viscosity changes, but little, with the initial value of $[\eta]$ and with the solution concentration in the range between 20 ppm and 4000 ppm. The limiting intrinsic viscosity coincides with the critical $[\eta]$, at which elasticity and shear-thinning of the solution come into being, and approximates $[\eta] = 280$ [19, 20].

The observations of samples prepared from dilute solutions of Polyox WSR-301 in isopropanol and of PIB in hexane showed that these solutions also contain fibrillar network structures, see Figs. 5 and 6.

Orientation of the fibrils in strong elongational flow can be illustrated by the following experiment. A drop of the PEO solution was placed between a pinched pair of pincers. When the pincers were opened, the drop was drawn into a liquid filament which was immediately

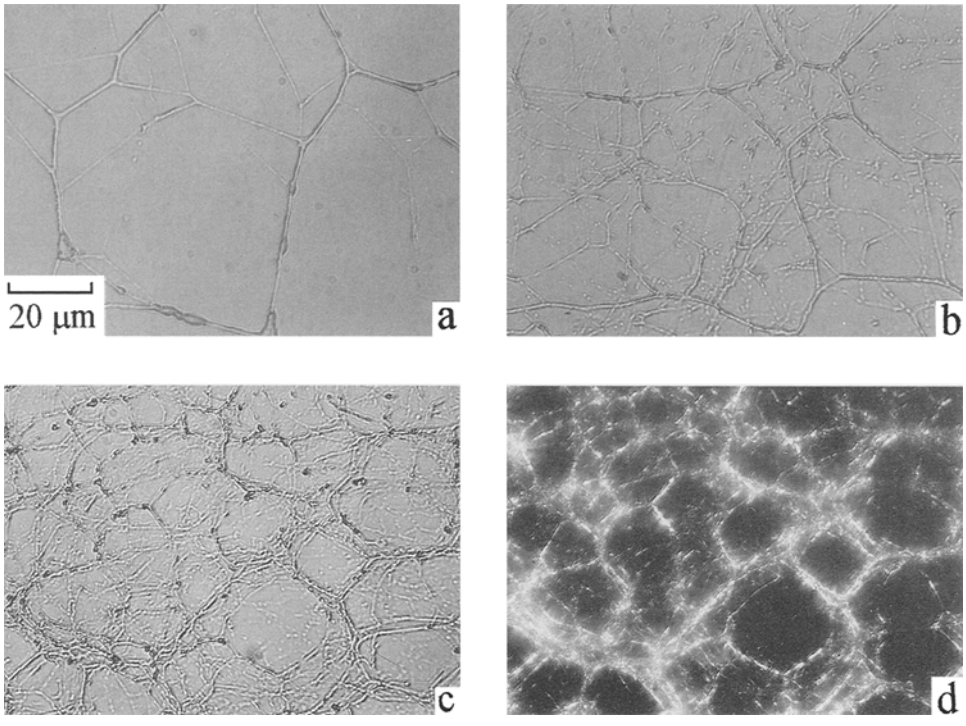

Fig. 2 Micrographs of the residues from freeze-dried aqueous solutions of Polyox WSR-301 $[\eta] = 2500$, as the concentration varies (using the method of rapid drying). a) – $c = 5$ ppm; b) – 25 ppm; c) – 100 ppm; d) – sample c), but between crossed polarizers

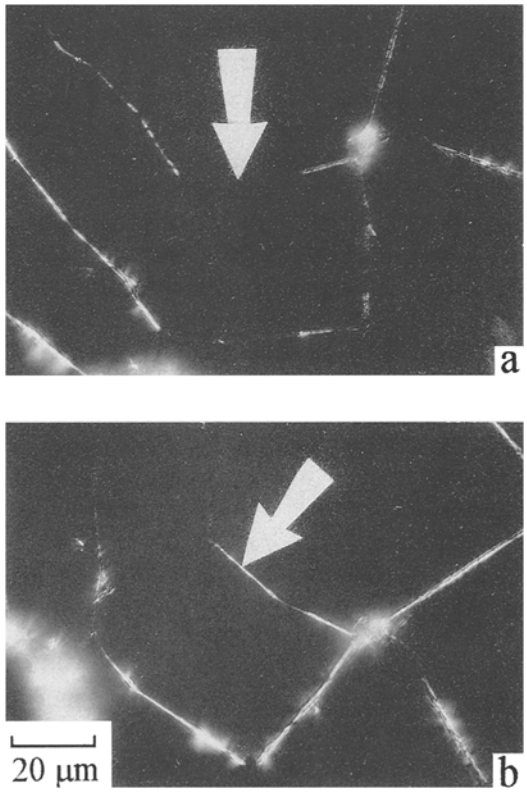

Fig. 3 Birefringence of fibrils from an aqueous solution of Polyox WSR-301 $[\eta] = 2500$, $c = 5$ ppm. The rapid drying method was used. Micrograph (b) is obtained after rotation of the crossed polars by an angle of 45 degrees

immersed into liquid nitrogen. The frozen filament was put on the glass plate and carried under liquid nitrogen into the vacuum chamber, where the sublimation of the solvent was performed. This procedure was aimed at preserving the network structure in a deformed state. The observation of this structure under the microscope showed that as a result of the extension of the liquid most fibrils became oriented along the filament, see Fig. 7.

Onset of flow birefringence

Flow birefringence experiments with cross-slot cells were run using aqueous solutions of PEO of various molecular weights and PIB in kerosene. The solution concentration and temperature were also varied. When the flow rate was increased until the strain rate attained its critical value at the center of the cross, a sharply confined birefringent line appeared in the outlet channels. At that moment the critical flow rate Q^* was measured. With further increase of flow rate, thickness, length and brightness of the line also increased. The observed picture closely resembled the one described in work [7]. Finally, birefringence lost its localization and subsequently became unstable. From this moment birefringence could be observed in the inlet as well as in the outlet channels. This pattern bears much resemblance to the "flare" phenomenon treated in work [18].

The concentration range within which Q^* could be measured for a solution of a certain polymer and a given

Colloid & Polymer Science, Vol. 274, No. 12 (1996)

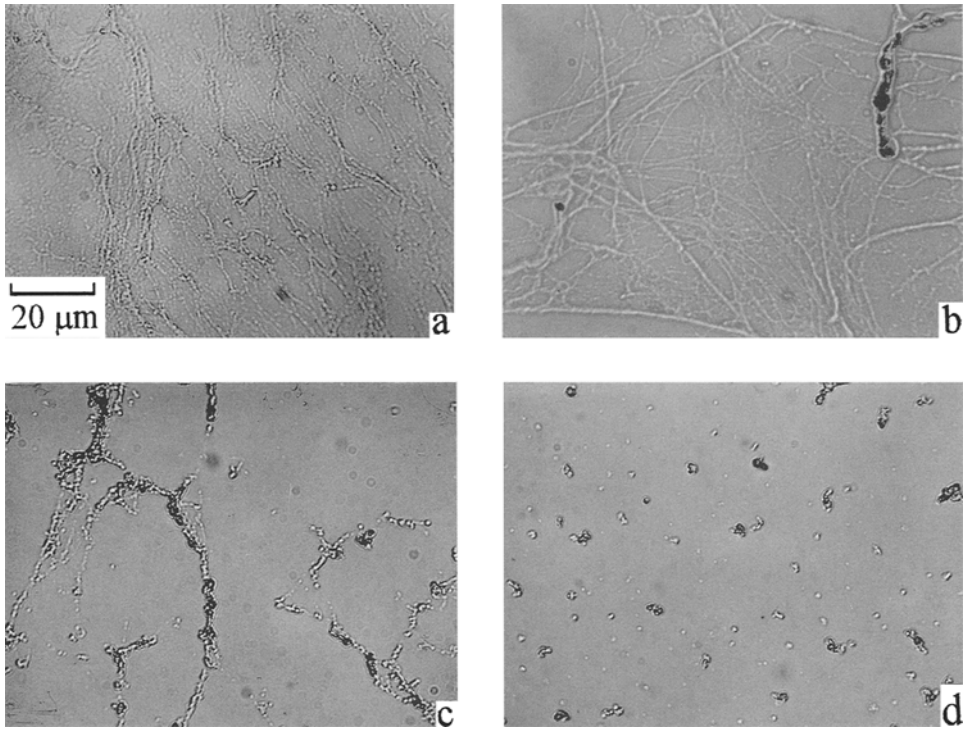

Fig. 4 Micrographs of the residues from freeze-dried aqueous PEO solutions $c = 10$ ppm, as the intrinsic viscosity varies (using the method of slow drying). a) – $[\eta] = 4500$, b) – 2500, c) – 450, d) – 90

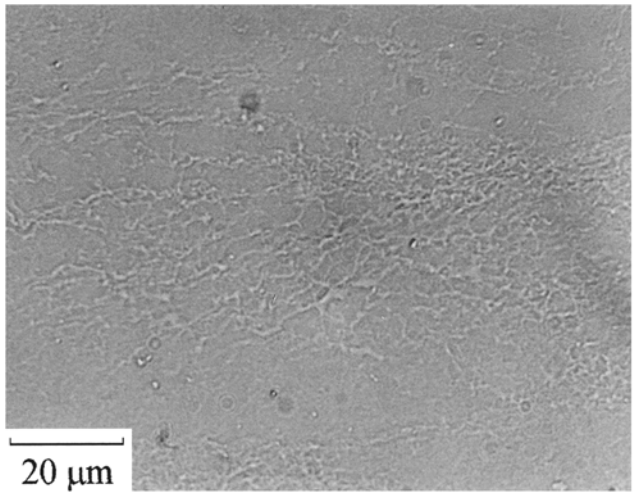

Fig. 5 Micrograph of the residue from a solution of Polyox WSR-301 in isopropanol, $c = 20$ ppm. The slow drying method was used

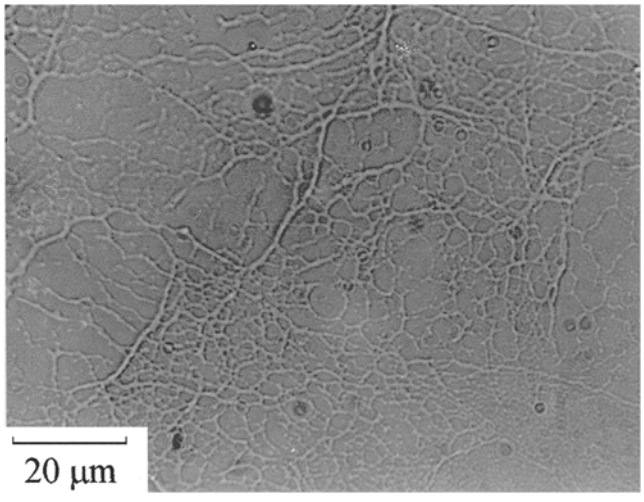

Fig. 6 Micrograph of the residue from a solution of PIB in hexan, $c = 20$ ppm. The slow drying method was used

temperature was quite narrow and did not exceed one order of magnitude. The lower concentration limit was determined by the hydrodynamic stability of the planar flow in the cell [32]. When the polymer concentration was decreased, the localized birefringence appeared at a higher flow rate. As a result, a moment was attained when the stability of the planar flow was lost before the birefringent line appeared. In this case, instead of a thin line we could only observe weak delocalized lightning. The larger the width of the slots d, the higher the concentration corresponding to the lower limit of the measurement interval. The upper limit of the concentration range was determined

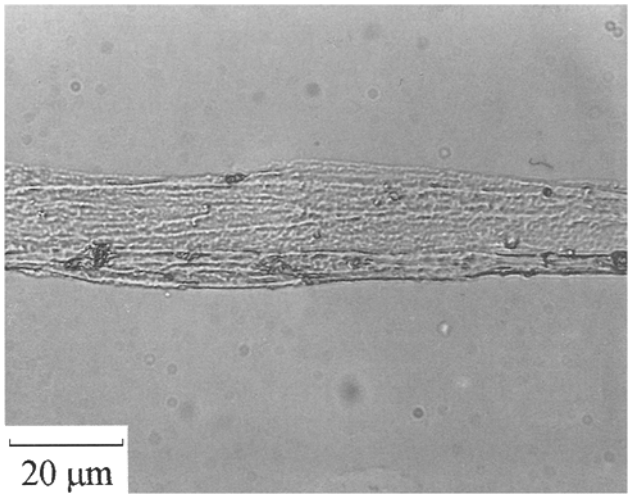

Fig. 7 Micrograph of the residue from a pre-extended and freeze-dried sample of aqueous solution of Alcox $[\eta] = 4500$, $c = 40$ ppm

by the formation of the persistent gel-like structures at the central part of the cross probably due to flow-induced crystallization, which significantly reduced the accuracy of the determination of Q^*.

From the measured value of Q^*, the value of the average velocity $V^* = Q^*/(2hd)$ was found. Figure 8 presents data on d/V^*, which, except for a constant factor, is the reciprocal of the extensional strain rate. For most solutions tested the direct proportionality between the value of d/V^* and $c^{1/2}$ seems to be a best fit. The deviation from this relationship was noticed only for the points correspondent to the most concentrated solutions of PEO.

In an attempt to relate the data on the critical extensional strain rate to the elastic properties of solutions, one can compare the curves of Fig. 8a with those of Fig. 1, where values of the natural time θ are presented for the same polymer solutions. The similarity between curves shown in these figures is quite clear. This fact suggests that the parameter which determines the onset of the localized birefringence is the Weissenberg number

$$We = \frac{\theta V}{d} = \frac{\theta Q}{2hd^2}.$$

The data of Fig. 9, where values of the critical Weissenberg number We^* are shown, support the above suggestion. The values of We^* were calculated from the data shown in Fig. 1, Table 1, and Fig. 8. The points corresponding to various polymer–solvent systems at different conditions are localized around a single value of $We^* = 1.1$.

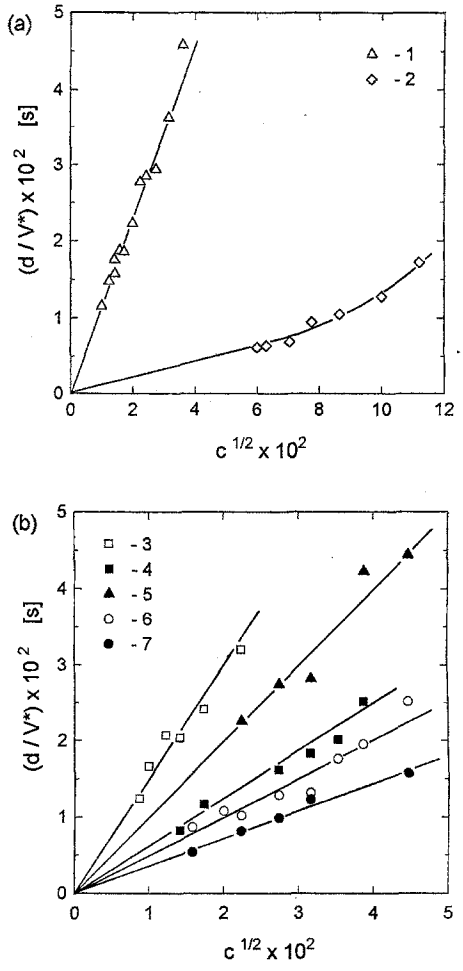

Fig. 8 The value of d/V^* against the one-half power of the concentration. PEO in water: $d = 0.49$ mm, 22 °C; $[\eta] = 790$ (2), $= 1000$ (6), $= 2500$ (1), $d = 0.49$ mm, $[\eta] = 2500$; 8.6 °C (3), 41.7 °C (4), $d = 0.80$ mm, $[\eta] = 2500$, 22 °C (5), PIB in kerosene: $d = 0.49$ mm, $[\eta] = 950$, 22 °C (7)

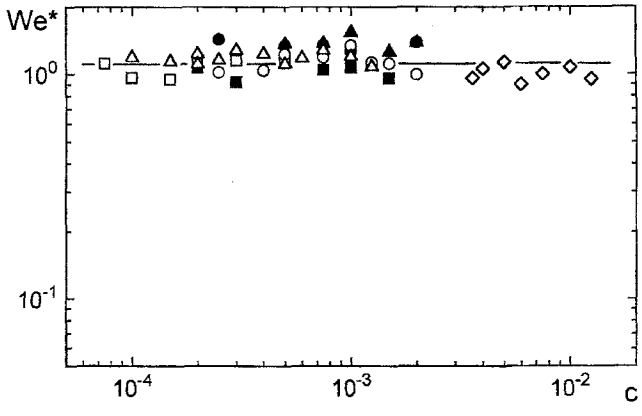

Fig. 9 Critical Weissenberg number determining the appearance of birefringence. Symbols as in Fig. 8

Colloid & Polymer Science, Vol. 274, No. 12 (1996)

Discussion

Reliability of interpretation

A problem of artefacts is frequently discussed in studies of supermolecular structures by observations of freeze-dried polymer solutions. Concern is sometimes expressed that the observed structures of the residue are not connected with the actual structures of the solution, but arise in the process of preparation as a result of the displacement of the polymer molecules to the boundaries of the crystals of solvent which are formed during freezing. In our opinion, the experiments that have been carried out dispel this concern. If it is assumed that the observed structure arises as a result of displacement of the polymer to the boundaries of crystals, then in this case the nature of the sample must depend on the conditions under which it was prepared. However, the structural differences observed in samples prepared both by rapid drying and by slow drying from the same solutions are of a minor nature. In the method of slow drying the solution droplets were submerged in liquid nitrogen, where the rate of cooling for the small droplets exceeds 100 °C/s. The further sublimation was carried out at a temperature of −80 °C. Under these conditions crystals of solvent were able to grow in crystallization or recrystallization processes only to very small sizes, not exceeding the typical size of the structures observed. In addition the fibrillar structures were also noticed for PEO solutions in isopropanol, which is known to vitrify under the rapid cooling.

The occurrence of a network in freeze-dried samples and the increase of its thickness are in good agreement with the occurrence and increase of the viscoelastic properties of the aqueous PEO solutions as the molecular weight of the dissolved polymer increases [19, 20], that would hardly be the case if the structures arose only in preparation of the sample. The aligned fibrils observed in experiment with stretching and freezing of the liquid filament of the PEO solution also support the notion that the picture which can be observed adequately represents the real structure of the polymer solutions.

The results of our experiments check well with those obtained previously [25–27]. However, we have to mention the dissimilarity of our data from the data on supermolecular structures in work [23], wherein fine spraying was applied in the course of specimen preparation for electron microscopy. The spray used yielded the droplets of a few micrometers in diameter, which could result in a collapse of the sizeable supermolecular formations.

Phase separation and bicontinuity

Microscopical study of freeze-dried samples supports ideas on the polymer solutions of interest as on two-phase systems. Polymer concentration of one phase is higher than of another. The volume fraction in solution of this polymer-rich phase is less than the volume fraction of the phase depleted in polymer. Depending on the characteristics of solution and dissolved polymer, the phase enriched in polymer may form either scattered globules or a three-dimensional network composed of interacting fibrils. In particular, transition from a network state to a globule state occurs with decreasing molecular weight of polymer (see Fig. 4). Further decrease of molecular weight will inevitably bring the solution to a single-phase state with molecular dispersity of polymer. It may be safely suggested that similar transition takes place when decreasing the polymer concentration. For the high-molecular weight polymers, this transition may occur at extremely low concentration that is several orders of magnitude less than c^*.

Birefringence of slender structures in the residues tells in favour of the crystalline nature of the fibrils in solutions. On the other hand, solutions under study do not display the yield stress and thixotropy. Therefore, the fibrils of these solutions must be taken as liquid–crystalline structures rather then stable, solidlike crystallites, as distinct from supermolecular structures in certain solutions of biopolymers [33]. The polymer-rich phase is a liquid both in the network state and in the globule state, as indicated by the solution capability to enter via very fine filters. As for the structure of the phase depleted in polymer, it can be suggested that polymer in this phase is dispersed in the form of separate molecules.

Only one phase occupies a connected space, when solutions carry the globules. In solutions with interacting fibrils, the phases are both placed within connected spaces of their own, which are percolated one through the other. In this case, we are dealing with the so-called equilibrium bicontinuous structures [34]. The bicontinuous structures are widely distributed in dispersions where they arise probably as the result of spinodal decomposition. The cytoplasm of the living cell is noteworthy [35]. Observations of this substance were conducted with the high-voltage electron microscope, which made it possible to watch the network structures within thick specimens or even within intact cells up to several micrometers thick, in so doing the removal of liquid from the object of observation was not necessary.

The drastic morphological changes which follow the transition from the globular to the bicontinuous state give rise to elastic and shear-thinning properties of the polymer solutions. These properties arise at the same value of the

intrinsic viscosity, at which the network appears. The considerable elastic properties associated with the bicontinuous structure lead to unusual hydrodynamic phenomena – the turbulent drag reduction and the increase of the pressure gradient in flow through a porous medium. The fact that the macromolecules in solutions suffer destruction also seems to be connected with the network structures; destruction arrests itself as soon as bicontinuity disappears. It is conceivable that the flocculating capability of the polymers in solutions is explained by bicontinuity and by formation of fibrillar bridges between solid particles [24].

Behaviour of fibrillar network in extensional flow

As with most of the known liquid–crystalline substances, the fibrillar networks are bound to be a viscoelastic continuum. That is the highly probable reason for the viscoelasticity of polymer solutions in which the network is present. Another plausible source of the solution elasticity is the surface tension on the phase boundary of the bicontinuous structure. In this regard the elasticity of the polymer solutions is analogous to the foam elasticity. In any event, in the extensional flow of high strain rate the fibrillar network is liable to behave like a network with fixed nodes, whose flexible links (fibrils) withstand significant stresses without noticeable extension. For this reason, the fibrils were oriented along the extension line and pulled together, thus expelling the solvent (more precisely, the phase depleted in polymer) from the network cells to the periphery of the liquid filament that was drawn by pincers. In a cross-slot flow, the fibrillar network supposedly acts in a similar way. In this case the fibrils are oriented along and confined to the symmetry plane of the exit channels, ejecting the solvent to the flow boundaries.

There is good reason to believe that the fibrils are primary birefringent elements in a dynamic birefringence phenomenon of solutions being studied. The flow-induced deformation of the liquid–crystalline fibrillar network and preferential spatial orientation of birefringent objects, such as fibrils, leads to integral birefringence in the flow. Specifically, it counts in favor of this conception that flow birefringence (much like elastic properties, shear thinning, drag reduction, and degradation) vanishes at the critical value of molecular weight or intrinsic viscosity, when the network disappears [7, 28].

Orientation is opposed by disordering effect of the thermal fluctuations, as well as by the stress relaxation in the fibrillar network. Therefore, orientation arises in a hydrodynamic field only at the sufficiently high strain rate when the liquid–crystalline part of the bicontinuous structure manifests itself as an elastic body. As the strain rate increases, this situation occurs when elastic forces become commensurable with viscous forces in the flow, or, in other words, when the Weissenberg number goes up to the order of unity, considering that this number is a measure of the elastic to viscous forces ratio [29].

Constriction of the network and displacement of the solvent must increase the polymer concentration in that part of flow where birefringence appears. This suggestion is confirmed by results in ref. [2], where the contrasting regions of increased concentration were observed in unpolarized light because of the difference of refractive indices between these regions and the surrounding liquid.

Boundary between the localized birefringent region and the remainder of the flow is a clear-cut one. Sharpness is also inherent in boundary of the above-mentioned contrasting region of increased concentration. However, the network constriction which occurs as a consequence of its extension by the flow, cannot serve as the only explanation for the existence of the distinct boundaries. In this connection, we would like to draw the reader's attention to the fact that the fibril orientation and the increased polymer concentration in extended regions are prerequisites for the occurrence of flow-induced crystallization supplementary to crystallization in the quiescent solution which is responsible for the formation of the fibrillar network.

Apparently a special role in the flow-induced crystallization is played by the cooperative effect of the cohesion forces between fibrils transferred into a parallel arrangement by the network extension. As a result, in the regions of high strain rates, a type of a dynamic liquid crystal can be formed. If the solution concentration is not high, this dynamic crystallization is reversible: After cessation of flow, the liquid–crystalline regions disappear at a certain rate depending on the concentration. In more concentrated solutions, the phenomenon acquires irreversible character, and persistent gels or even solid crystallites can be formed which do not disappear after flow is stopped.

A noticeable change in the velocity profile is observed in the outlet flows, which accompanies birefringence [36, 37]. For the highly birefringent region, a local minimum at the midpoint of the velocity profile is observed. This depression in the profile can be explained in a reasonable way with regard to the additional drag arising at high strain rate from the presence of the fibrillar network, which is here extended and formed the supermolecular structure that has a higher level of organization than fibrils. Broadly speaking, it is hoped that the allowance made for the existence of the fibrillar network can be helpful when analyzing results of a large body of literature dealing with the flow-induced association and crystal formation investigated, not only in connection with flow birefringence [2, 10–12], but independently as well [38–46].

The above views regarding orientation, increase of concentration, solvent exclusion, and gelation are in general agreement with those given in work [45]. The distinction lies in the fact that the authors of the cited work believe that cross-links between limited number (as a rule, between two) adjacent chain segments can take place in solutions during rest. In particular, it is their opinion that orientation not only of the cross-linked but also separate segments of macromolecules occurs in elongational flow. In contrast to this, the data of microscopy points to the fact that attraction forces between polymer chains may result in the fibrils involving a large number of macromolecules. Integrated in a network, these fibrils show a great capacity for orientation in elongational flow and are bound to play a dominant role in phenomena being discussed.

Acknowledgments The International Science Foundation (Grants ME69000 and ME69300) is gratefully acknowledged for financial support in the final stage of this work.

References

1. Tsvetkov VN, Eskin VW, Frenkel SY (1964) Structure of Macromolecules in Solutions. Nauka, Moscow [(1971) Vol 3. National Lending Library for Science and Technology, Washington]
2. Frank FC, Keller A, Mackley MR (1971) Polymer 12:467–473
3. Frank FC, Mackley MR (1976) J Polym Sci Polym Phys Ed 14:1121–1131
4. Cressely R, Hocquart R, Scrivener O (1976) Optica Acta 26:1173–1181
5. Crowley DG, Frank FC, Macley MR, Stephenson RG (1976) J Polym Sci Polym Phys Ed 14:1111–1119
6. Berry MV, Mackley MR (1977) Philos Trans R Soc London A 287:1–16
7. Scrivener O, Berner C, Cressely R, Hocquart R, Sellin R, Vlachos NS (1979) J Non-Newton Fluid Mech 5:475–495
8. Cressely R, Hocquart R (1980) Optica Acta 27:699–711
9. Pope DP, Keller A (1978) Colloid Polym Sci 256:751–756
10. Mackley MR, Keller A (1975) Philos Trans R Soc London A 278:29–66
11. Fuller GG, Leal LG (1981) J Polym Sci Polym Phys Ed 19:557–587
12. Torza S (1975) J Polym Sci Polym Phys Ed 13:43–57
13. Carpenter DK, Santiago G, Hunt AH (1974) J Polym Sci Polym Symp 44:75–82
14. Barenblatt GI, Bulina IG, Zel'dovich YaB, Kalashnikov VN, Sholomovich GI (1965) Zh Prikl Mekh Tech Fiz 5: 147–148 [(1965) J Appl Mech Tech Phys 5:103–104]
15. Barenblatt GI, Kalashnikov VN (1968) Izv Akad Nauk SSSR Mekh Zhidk Gaza 3:68–73
16. Dunlope EH, Cox LR (1977) Phys Fluids 20(2):S203–S215
17. Berman NS (1980) Polym Eng Sci 20: 451–455
18. Keller A, Müller AJ, Odell JA (1987) Progr Colloid Polym Sci 75:179–200
19. Kalashnikov VN, Askarov AN (1989) Inzh-Fiz Zh 57:198–203 [(1989) J Eng Phys 57:874–878]
20. Kalashnikov VN (1994) J Rheol 38: 1385–1403
21. Hambraeus G, Ránby B (1945) Nature 155:200–201
22. Kargin VA, Bakeev NF (1957) Kolloid Zh 19:133–137
23. Richardson MJ (1964) Proc R Soc London A 279:50–61
24. Audsley A, Fursey A (1965) Nature 208:753–754
25. Ouibrahim A (1978) Phys Fluids 21:4–8
26. James DF, Saringer JH (1980) J Fluid Mech 97:665–671
27. Miyamoto H, Ando T (1989) Jpn Soc Mech Eng B 55:3391–3396
28. Kalashnikov VN, Tsiklauri MG (1990) Inzh-Fiz Zh 58:49–55 [(1990) J Eng Physics 58:40–45]
29. Astarita G, Marrucci G (1974) Principles of Non-Newtonian Fluid Mechanics. McGraw Hill, London
30. Kalashnikov VN, Askarov AN (1987) Inzh-Fiz Zh 53:573–579 [(1987) J Eng Physics 53:1140–1144]
31. Kalashnikov VN (1987) In: Struminski VV (ed) Problems in Turbulent Flows. Nauka, Moscow, pp 163–171 [(1988) Fluid Mech – Soviet Research 17: 80–92]
32. Kalashnikov VN, Tsiklauri MG (1993) J Non-Newton Fluid Mech 48:215–223
33. Giordano R, Mallamace F, Micali N, Wanderlingh F, Baldini G, Doglia S, (1983) Phys Rev A 28:3581–3588
34. Scriven LE (1977) In: Mittal KL (ed) Micellization, Solubilization, and Microemulsion. Vol 2. Plenum Press, New York and London, pp 877–894
35. Wolosewick JJ, Porter KR (1979) J Cell Biology 82:114–139; Porter KR, Tucker JB (1981) Sci Amer 244:57–67
36. Lyazid A, Scrivener O, Teigen R (1980) In: Astarita G, Marrucci G (eds.) Rheology. Vol 2. Plenum Press, New York, pp 141–148
37. Gardner K, Pike ER, Miles MY, Keller A, Tanaka K (1982) Polymer 23: 1435–1442
38. Pennings AJ, Kiel AM (1965) Kolloid-Z Z Polym 205:160–162
39. Giesekus H (1969) Rheol Acta 8: 411–421
40. Pelzbauer Z, St John Manley R (1970) J Macromol Sci Phys B 4:761–774
41. Zwijnenburg A, Pennings AJ (1975) Colloid Polym Sci 253:452–461; (1976) 254: 868–881
42. Metzner AB, Cohen Y, Rangel-Nafaile C (1979) J Non-Newton Fluid Mech 5: 449–462
43. James DF, Saringer JH (1982) J Non-Newton Fluid Mech 11:317–339
44. Rangel-Nafaile CA, Metzner AB, Wissbrun KF (1984) Macromolecules 17: 1187–1195
45. Ferguson J, Hudson NE, Warren BCH (1987) J Non-Newton Fluid Mech 23: 49–72
46. McHugh AJ, Spevacek JA (1991) J Polym Sci B 29:969–979